Annales Societatis Geologorum Poloniae (2024), vol. 94: 329–344 https://doi.org/10.14241/asgp.2024.15

THERMAL HISTORY OF THE NORTHERN MARGIN OF THE HOLY CROSS MOUNTAINS (POLAND) FROM THE CARBONIFEROUS TO THE MESOZOIC, BASED ON VITRINITE REFLECTANCE DATA: VARISCAN VERSUS POST-VARISCAN EVENTS

Dariusz BOTOR

AGH University of Kraków, Faculty of Geology, Geophysics and Environmental Protection, 30–059 Kraków, Mickiewicza 30, Poland,
e-mail: botor@agh.edu.pl

Botor, D., 2024. Thermal history of the northern margin of the Holy Cross Mountains (Poland) from the Carboniferous to the Mesozoic, based on vitrinite reflectance data: Variscan versus post-Variscan events. *Annales Societatis Geologorum Poloniae*, 94: 329–344.

Abstract: Vitrinite reflectance analysis was applied to establish the burial and thermal history of the northern margin of the Holy Cross Mountains. The open public mean random vitrinite reflectance (VR) data were analysed in four borehole sections (Opoczno PIG-2, Ostałów PIG-2, Nieświń PIG-1, and Radwanów IG1). Non-linear VR patterns in the Permian–Triassic strata suggest that thermal maturity developed due to hot fluid flow in the Jurassic. Additionally, in three well sections, VR breaks occur at the base of the Permian. Therefore, the thermal maturity of the organic matter, contained in the Carboniferous strata, was reached at the end of the late Carboniferous and was not overprinted by Mesozoic processes. Both sedimentary burial and fluid-flow processes could contribute to a high level of thermal maturity of the Carboniferous rocks. In summary, this work: (1) highlights the influence of hydrothermal events in the Mesozoic on thermal maturity patterns; (2) extends the earlier observations of the late Variscan (pre-Zechstein) thermal event/regime beyond the Małopolska Block onto the Łysogóry Block; and (3) discards the influence of Permian-Mesozoic burial on the maturity of Carboniferous and, by implication, older strata.

Keywords: Vitrinite reflectance, thermal history, Holy Cross Mountains, Polish Basin.

Manuscript received 16 January 2024, accepted 10 December 2024

INTRODUCTION

Understanding the burial and thermal history within sedimentary basins is essential for a range of fundamental and applied purposes (Laughland and Underwood, 1993; Schegg and Leu, 1998; Mazurek, *et al.,* 2006; Sakaguchi *et al.,* 2007; Hantschel and Kauerauf, 2009; Cavailhes *et al.,* 2018; Suchý *et al.,* 2019). Temperature evolution in the uppermost crust and, hence, in a sedimentary basin is mainly controlled by tectonic processes (e.g., McKenzie, 1981). The thermal maturity pattern of organic matter is widely applied to reconstruct the thermal history of sedimentary basins and to validate thermal maturity modelling (Hantschel and Kauerauf, 2009; Suchý *et al.,* 2019). The mean random vitrinite reflectance (VR) determination method now is widely used to establish the thermal maturity of coal and dispersed organic matter in fine-grained rocks (Suarez-Ruiz *et al.,* 2012). An increase in VR value depends on many parameters, including temperature, geological time, pore fluid pressure, fluid chemistry, and the extent of tectonic deformation, causing maximum burial (Barker and Pawlewicz, 1994; Huang, 1996; Dalla Torre *et al.,* 1997), of which the most important are the influence of the maximum temperature and the duration of heating (Mukhopadhyay, 1992).

An important issue, when reconstructing the burial history of a study area, is the thickness of exhumed sediments. The extent of the Variscides in central and southern Poland recently has been disputed (Krzywiec *et al.,* 2017a, b; Mazur *et al*., 2020; Narkiewicz, 2020). The range of the Variscides near the Holy Cross Mountains (HCM) area was originally determined by Pożaryski *et al.* (1992), who located this front in the immediate vicinity of the Palaeozoic core of the HCM, while Dadlez *et al.* (1994) assumed that

the Variscan front had occurred farther west. The results of the research on Carboniferous sediments in the Opoczno PIG-2, Ostałów PIG-2 and Studzianna IG-2 wells are of key importance for these interpretations. In the study area, there is a Carboniferous siliciclastic complex of several hundred metres (Krzemiński, 1999). Sedimentary structures resemble those of a flysch sediment complex but, in a genetic sense, the sequence does not fully meet the conditions for such a classification (Jaworowski, 2002). The early Carboniferous (Tournaisian–Visean; Turnau, 1999) age of the analysed sediments is almost equal to that of the Culm facies, known from the southern part of the HCM (Żakowa and Migaszewski, 1995), as well as the Moravo-Silesian fold-and-thrust belt sediments, known from NE Czechia and SW Poland (Kalvoda *et al.,* 2008). Comprehensive analysis of the described rocks allows location of the Variscan front to the west of a line between the Studzianna IG-2 and Ostałów PIG-2 wells. However, Krzemiński (1999) placed it relatively close to a line between the Budziszewice IG-1 and Radwanów IG-1 wells, while Jaworowski (2002) moved the Variscan front farther west. Therefore, there is no consensus regarding the position of the Variscan front in this area, which could have produced additional heating due to tectonic burial in the study area. The purpose of this work is a comprehensive analysis of the thermal maturity of organic matter, in order to explain the burial and thermal history of the study area. In this work, the published VR measurements performed by Swadowska (2006a, b) and Grotek (2018) are analysed, in order to explain the thermal evolution of the study area. In addition, VR data from the Radwanów IG-1 well is also used (Łuszczak *et al.,* 2020). The VR analysis allows an insight into the thermal evolution of the northern margin of the HCM.

GEOLOGICAL SETTING

The study area is located within the northern margin of the HCM (Fig. 1), which was formed during the Late Cretaceous–Palaeogene tectonic inversion of the Permian–Mesozoic Polish Basin in its SE part (Kutek and Głazek, 1972; Dadlez *et al.,* 1995; Krzywiec, 2002; Krzywiec *et al.,* 2018). The most subsiding (axial) part of the Polish Basin (the Mid-Polish Trough) evolved along the Teisseyre-Tornquist Zone (TTZ; see Mazur *et al.,* 2015, 2021 for a recent summary). Tectonic inversion of the Polish Basin was associated with uplift and exhumation of the axial part of the basin (Kutek and Głazek, 1972; Dadlez *et al.,* 1995; Krzywiec, 2002; Krzywiec *et al.,* 2018; Mazur *et al.,* 2015, 2021). The Polish Basin consists of an extensive Permian-Mesozoic succession, which is overlain unconformably by up to 350 m of poorly consolidated Cenozoic sediments (Piwocki, 2004). The Permian to Cenozoic sediments reach about 8 km in total thickness along a NW–SE-oriented depocentre in the Mid-Polish Trough (Dadlez *et al*., 1995; Lamarche *et al.,* 2003a, b; Mazur *et al.,* 2005, 2021).

The Palaeozoic core of the HCM comprises Cambrian to early Carboniferous sediments (Fig. 1) that were exhumed from beneath a Permian–Mesozoic cover during the Late Cretaceous inversion of the Polish Basin (Lamarche *et al.,* 1999, 2003a, b; Mazur *et al.,* 2005; Krzywiec, 2009). The Palaeozoic strata of the HCM occur on both sides of the Holy Cross Fault (HCF), which is the boundary between the Łysogóry and Małopolska Blocks (Fig. 1). In a pre-Permian section of analysed wells, only the lower Carboniferous strata were identified, ranging from upper Tournaisian to early Visean, which are covered by Permian and Mesozoic sediments (Kowalczewski, 2006a, b; Fijałkowska-Mader, 2018). The minimum primary thickness of the lower Carboniferous is estimated at c. 300 to 800 m in the Kielce Unit and is rather poorly constrained, due to repeated erosion and a lack of continuous sections (Narkiewicz *et al.,* 2010). From the early Bashkirian (late Namurian A), non-deposition and erosion dominated the entire Variscan foreland area (Narkiewicz, 2020). Several magma pulses occurred in the HCM and their time frame was determined by means of K-Ar and $^{40}Ar/^{39}Ar$ geochronology (Migaszewski, 2002; Nawrocki *et al.,* 2013), as well as zircon U-Pb dating (Krzemińska and Krzemiński, 2019). Firstly, late Silurian to Early Devonian magmatic events were deciphered from zircons in the Kielce Unit (425.7 Ma and 414.5 Ma). Secondly, extensive late Variscan magmatism in the Kielce and Łysogóry Units occurred at 322 Ma and at 300 Ma, respectively, when the lamprophyre of Podkranów (Kielce Unit) and diabase of Milejowice (Łysogóry Unit) were emplaced, coevally with the silicic igneous magmatism at the southern margin of the Małopolska Block (Słaby *et al.*, 2010). This documents the synchronicity of magmatic events in both domains (Krzemińska and Krzemiński, 2019). According to Lamarche *et al*. (2003a), the longitudinal discontinuities represent inverted normal faults that developed due to the Devonian extension. The palaeomagnetic results impose wide constraints on the timing of the late Palaeozoic deformation of the HCM: from the Visean–Serpukhovian boundary (c. 331 Ma), when an early folding phase occurred, to the early Permian marking the termination of the Variscan tectonism (Lamarche *et al.,* 2003a; Szaniawski, 2008; Narkiewicz, 2020).

In the HCM, the Variscan erosional surface is overlain by 200 m of Permian sediments, including the locally preserved Rotliegend siliciclastic and Zechstein evaporite deposits (Żakowa and Migaszewski, 1995). Subsequent rapid sedimentation continued in the Mesozoic, leading to the deposition of approximately 2.0–3.5 km of epicontinental deposits (Kutek and Głazek, 1972; Kutek, 2001). The lowermost part of the Triassic succession comprises clastic sediments: conglomerates, sandstones, mudstones and claystones (Kuleta and Zbroja, 2006). The Lower Triassic strata are covered by Middle Triassic carbonates and claystones. The Upper Triassic sequence comprises claystones and mudstones with intercalations of sandstones, marls, dolomites, anhydrite and gypsum (Kowalczewski, 2006a, b). The Lower Jurassic sequence is largely represented by terrestrial clastic rocks, such as conglomerates and sandstones (Pieńkowski, 2004). The Middle Jurassic strata are composed of clastic marine sediments, such as clays, sandstones, siltstones and limestones. The Upper Jurassic rocks comprise Oxfordian and Kimmeridgian limestones and clayey marls (Kutek, 1968; Matyja, 1977). The Upper Jurassic rocks are overlain by Lower Cretaceous sandstones, calcareous

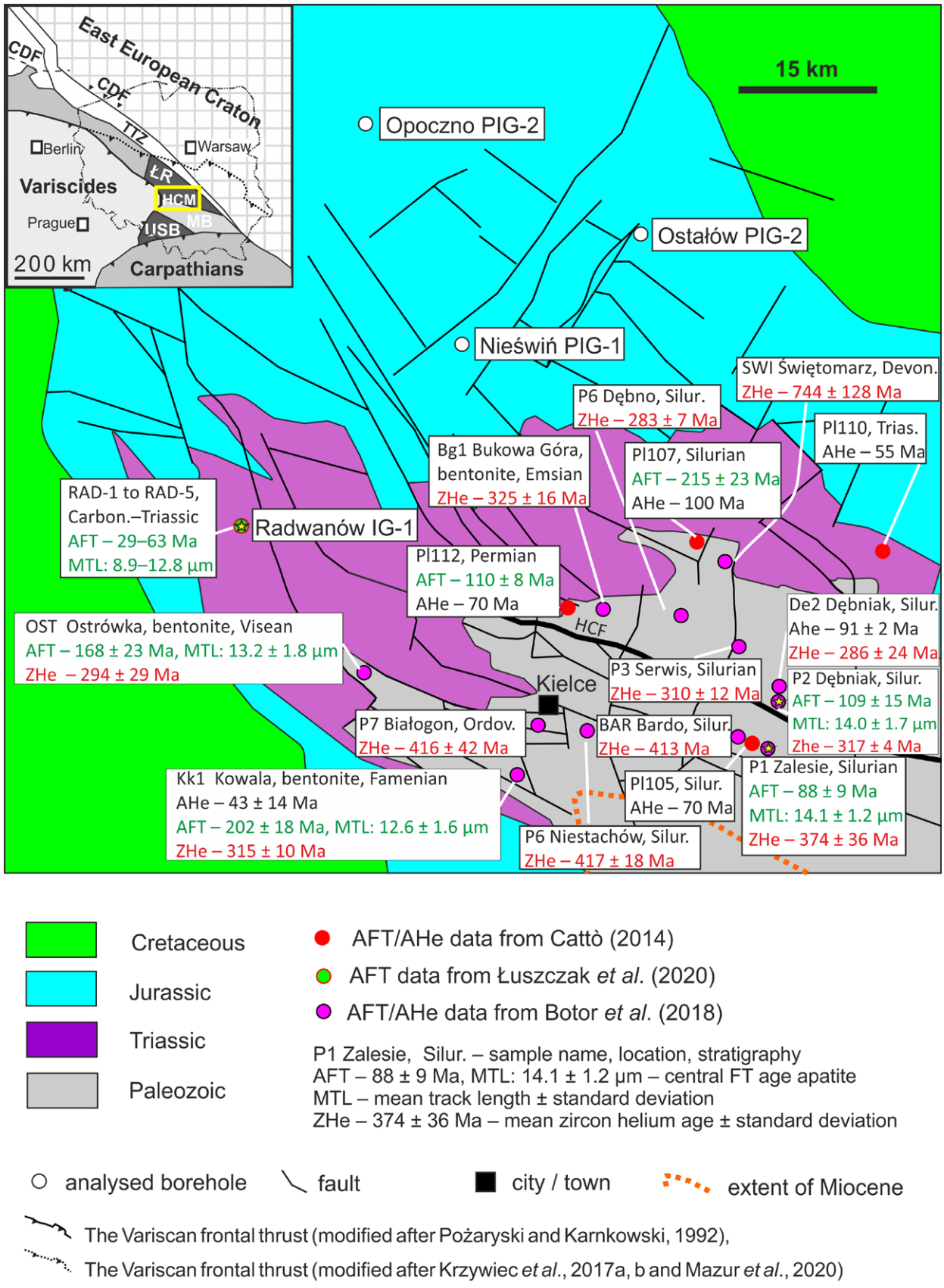

Fig. 1. Location of the analysed boreholes on a simplified geological map of the study area without Cenozoic deposits (after Dadlez *et al.,* 2000; modified). Lithology of the samples with zircons and/or apatites is sandstone, otherwise bentonite, as given in the text box. The inset in the upper left-hand corner shows pre-Permian regional tectonic elements (CDF: Caledonian Front, MB: Małopolska Block, ŁR: Łysogóry Region, USB: Upper Silesia Block, HCM: Holy Cross Mountains, TTZ: Teisseyre-Tornquist Zone). Yellow rectangle in the inset map marks the study area and outline of the geological map.

sandstones and spongiolites (Kowalczewski, 2006a, b). The Upper Cretaceous rocks consist of limestones, sandstones, conglomerates, clays, siliceous limestones, marls and calcareous sandstones that are Turonian to Maastrichtian in age. Continuous sedimentation in the Mesozoic was interrupted several times by small sedimentary gaps, of which the largest occurred in the Lower Cretaceous (Hakenberg and Świdrowska, 1998). This Hauterivian to Aptian/early Albian event was caused by the uplift and exhumation of c. 200 m of sediments (Hakenberg and Świdrowska, 1998). Due to tectonic inversion in the Late Cretaceous, significant exhumation of the Mesozoic rocks occurred, which led to the exposure of Triassic and Jurassic rocks, and even Palaeozoic basement rocks in the HCM (Fig. 1). The compressional/transtensional stress regime that triggered the inversion was caused by a combination of two mechanisms: the collisional phases in the Alpine and Carpathian orogens and the Atlantic opening (Dadlez *et al.,* 1995; Ziegler and Dèzes, 2007). Since neither Palaeogene nor Neogene deposits have been encountered in the northern and central parts of the HCM, it is assumed that the study area underwent continuous erosion during the Cenozoic (Kutek and Głazek, 1972; Jarosiński *et al.,* 2009).

PREVIOUS THERMAL HISTORY RESEARCH

In the area of the HCM, various thermal maturity indicators, such as the colour alteration index of conodonts (CAI), biomarkers, acritarchs, VR, and Rock-Eval pyrolysis, were studied (Bełka, 1990; Narkiewicz, 1991; Grotek, 1998; Szczepanik, 1997, 2001; Marynowski, 1999; Marynowski *et al.,* 2001, 2002; Narkiewicz and Malec, 2005; Malec *et al.,* 2010; Smolarek *et al.,* 2014; Malec, 2015). The data indicate that the thermal maturity of Palaeozoic rocks was reached much earlier than the Late Cretaceous, probably in the late Carboniferous. The thermal maturity pattern in the pre-Permian and younger rocks highlights the decisive role of high heat flow during the late Palaeozoic (Bełka, 1990; Marynowski, 1999; Narkiewicz *et al.,* 2010; Narkiewicz, 2017). In particular, the Carboniferous–Permian advective heat flow, related to fluid migration, was one of the major factors of thermal evolution (Poprawa *et al.,* 2005; Narkiewicz *et al.,* 2010, Naglik *et al.,* 2016). It seems that the HCF polyphase subsidence and burial were important for thermal maturation (Bełka, 1990; Marynowski, 1999; Poprawa and Żywiecki, 2005; Poprawa *et al.,* 2005). The Variscan deformation in the Carboniferous, due to tectonic overburden, might have caused an additional temperature increase and affected the thermal maturity of the organic matter (Lamarche *et al.,* 2003a; Narkiewicz, 2007). A late to post-Variscan cooling event of the Palaeozoic sequences, recorded by zircon helium ages (ZHe; Botor *et al.,* 2018), marks the end of an important thermal overprint, which is likely to be related to Variscan tectonics (Lamarche *et al.,* 1999, 2003a; Mizerski, 2004; Konon, 2006).

Consideration of only the maximum heating in the Jurassic and/or Cretaceous (as proposed by Poprawa *et al.* (2005) and Schito *et al.* (2017) is not plausible with the ZHe ages of Palaeozoic samples (Botor *et al.,* 2018). Alternative models accepted by some authors (Bełka, 1990; Marynowski, 1999; Narkiewicz, 2002; Narkiewicz *et al.,* 2010) assume that the main heating of the Devonian to early Carboniferous sedimentary successions occurred in the late Carboniferous (c. 330–299 Ma) and the early Permian (c. 299–280 Ma), except in the Kajetanów area, where an additional thermal event (c. 250 Ma) before the Middle Triassic was suggested by Marynowski *et al.* (2002). In the Mesozoic, the increase in temperature across most of the HCM area was connected to the subsidence of the Mid-Polish Trough and the resulting sedimentary burial. The central part of the HCM reveals a final fast cooling event, related to tectonic inversion of the Polish Basin (Dadlez *et al.,* 1995; Krzywiec, 2002; Lamarche *et al.,* 2003a, b). This cooling started in the Cenomanian to early Campanian (c. 100–90 Ma) at Łysogóry (Fig. 2) and c. 90 Ma, in the Kielce Unit (Botor *et al.,* 2018), as well as 91–82 Ma in the Radwanów IG-1 section (Łuszczak *et al.,* 2020). Such a fast-cooling event is also indicated by a small difference between the apatite fission-track (109 Ma) and apatite helium ages (91 Ma) in samples from the Dębniak outcrop in the central part of the HCM (Botor *et al.,* 2018). However, this event was much less marked on the SW margin of the HCM (the Kowala and Ostrówka area), where slow cooling continued throughout the Mesozoic, with only a minor acceleration of the cooling rate after the Late Cretaceous (Fig. 2; Botor *et al.,* 2018). Thermochronological data in Cattò (2014) also showed slow cooling in the northern part of the Łysogóry unit.

In the adjacent area SW of the HCM (the borehole sections of the Miechów Trough), the relatively low conodont CAI values of 1 in the Triassic rocks indicate that the Devonian and lower Carboniferous sediments must have reached their thermal maturity earlier, most likely in the late Carboniferous (Malec, 2015). Regionally distributed, low thermal maturity data (below 0.5% VR) in Mesozoic sediments also suggest pre-Triassic maturation of the Palaeozoic organic matter (e.g., Marynowski *et al.,* 2007). Miocene sediments in the Carpathian Foredeep also have low thermal maturity (below 0.5% VR, Szafran and Wagner, 2000). Conodont CAI data from the Silurian strata on the SW margin of the Małopolska Block display a relatively uniform thermal overprint (CAI values of 4), probably resulting from maximum burial in the late Carboniferous. The estimated maximum temperatures of c. 200 °C can be explained by an elevated heat flow, with a palaeogeothermal gradient of c. 60–70 °C/km, associated with the Kraków-Lubliniec Fault Zone. This thermal maturation level was locally enhanced (CAI values up to 8) in the late Carboniferous to early Permian (c. 300 Ma), due to magmatic and hydrothermal activity (Bełka and Siewniak-Madej, 1996).

METHODS AND DATA

One of the most frequently used methods of thermal history analysis is the numerical modelling of heat flow in the past burial history, which has proved to be an essential tool for petroleum exploration (Waples *et al.,* 1992a, b).

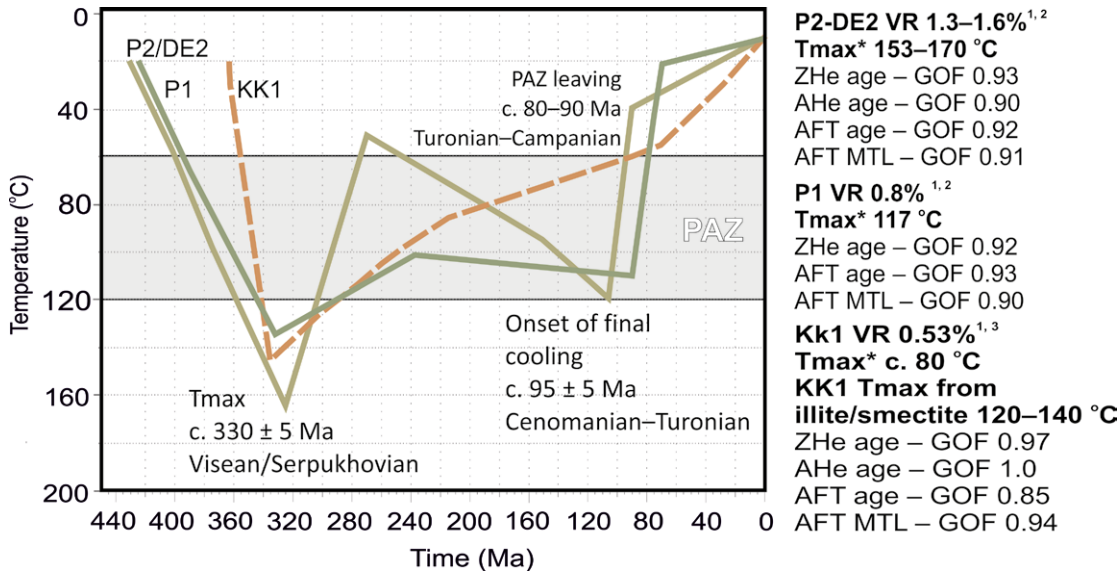

Fig. 2. The best fit curves, based on thermal modelling of apatite fission track and zircon helium data, applying HeFTy software (Ketcham, 2005) for Palaeozoic samples from the HCM area (after Botor *et al.,* 2018, modified). PAZ – Partial Annealing Zone of fission tracks in apatite (ca. 60–120 °C). Maximum temperature (Tmax) from illite/smectite data from Środoń and Trela (2012). VR-derived Tmax* based on Barker and Pawlewicz's (1994) approach for burial-induced temperature. VR data from: 1. Smolarek *et al*. (2014), 2. Schito *et al*. (2017), 3. Marynowski *et al*. (2001). Ordovician to Silurian samples close to HCF (P1, P2/DE2) show Late Cretaceous rapid cooling record on both sides of Holy Cross Fault (HCF), whereas there was no rapid cooling of Late Devonian samples at a distance from the HCF (KK1). Rapid cooling along the HCF can be attributed to the Late Cretaceous tectonic inversion of the HCM part of the Mid-Polish Trough. Further explanations are given in the text.

However, the validity of such models depends on the quality of the input data, which incorporates the exact stratigraphical thickness and thermal conductivity of individual layers (Waples *et al.,* 1992a, b). By far the most widely used data for calibrating these models are measurements of the VR, which can be compared with modelled reflectance values (Sweeney and Burnham, 1990).

Thermal maturity modelling was performed using PetroMod 1-D software (Schlumberger). The modelling procedure typically starts with a conceptual model, based on the geological evolution of the basin, including deposition, non-deposition, and erosion/exhumation. Input data also include the petrophysical parameters of a given lithology and present-day thermal regime (Hantschel and Kauerauf, 2009). In order to obtain a good fit between measured and calculated vitrinite reflectance values, different burial and heat flow scenarios were calculated by means of an iterative method using the EASY %Ro algorithm (Sweeney and Burnham, 1990). A broader discussion of the applied maturity modelling method was provided by Waples *et al*. (1992a, b) and Hantschel and Kauerauf (2009). However, because the thermal modelling approach was not successful in the case of the analysed wells, the time-independent approach (Barker and Pawlewicz, 1994) was applied. A major reason for the failure of PetroMod is the nature of heat transfer in the crust. In the PetroMod software, a conductive method is applied, which is not capable of simulating the hydrothermal processes that probably occurred in the study area. The thermal modelling approach was coupled with empirical studies in this work, as proposed in Barker and Pawlewicz (1994). In contrast to the traditional concepts that consider organic maturation to be a function of both maximum burial temperature and effective heating time (e.g., Hantschel and Kauerauf, 2009), the time-independent approach (Barker and Pawlewicz, 1994) has gained general acceptance for reconstructing the thermal histories of areas, characterized by complex geological histories (Barker, 1983*;* Barker and Pawlewicz, 1994; Akande and Erdtmann, 1998; Frings *et al.,* 2004; Cavailhes *et al.,* 2018). While the application of time-temperature models is limited to first-cycle sedimentary basins with well-known burial and thermal histories, the time-independent method, based on several statistical correlations between vitrinite reflectance and peak temperature, can be applied to complicated orogenic sequences (Laughland and Underwood, 1993) and hydrothermal systems (Barker, 1983). Correlations between fluid-inclusion homogenization temperature and vitrinite reflectance confirm that temperature is the major control of organic maturation (Tobin and Claxton, 2000*;* Barker and Pawlewicz, 1994). In this approach, VR is used as an input parameter for the estimation of maximum palaeotemperature (Barker and Pawlewicz, 1994). In the present study, the equation Temperature 1 = (lnVR + 1.68)/0.0124 was used for the burial heating model and Temperature 2 = (lnVR + 1.19)/0.00782 was used for the hydrothermal heating model, after Barker and Pawlewicz (1994). Based on VR data, the construction of isoreflectance lines is commonly used to estimate coalification gradients for stratigraphic successions, dominated by burial diagenesis. In such cases, isoreflectance lines should run parallel or sub-parallel to the bedding (Yamaji, 1986). Palaeogeothermal gradients can be determined by converting the VR data into temperature values. Several empirical

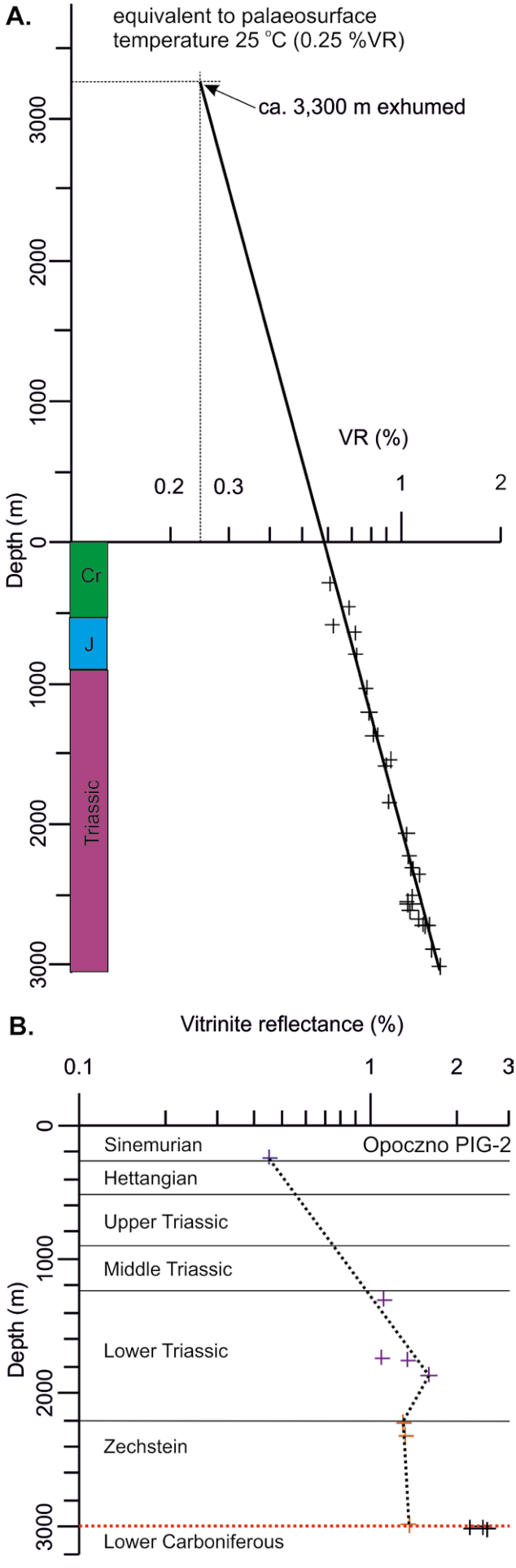

equations and methods have been presented, based on various assumptions and correlations, each with a varying emphasis on the importance of time and temperature during the coalification process (Barker and Goldstein, 1990; Sweeney and Burnham, 1990; Barker and Pawlewicz, 1994). The calculation of palaeogeothermal gradients and knowledge of the maximum thermal maturity allows for the estimation of the thickness of the eroded overburden.

The palaeogeothermal gradient is applicable to the time immediately before the onset of cooling from maximum palaeotemperatures. Calculating the amount of the eroded section from thermal data requires either: detailed knowledge of the lithologies of the removed section or assumptions about either the thermal conductivity and heat flow variation or the palaeogeothermal gradient through the missing section. In the absence of this information, and if the palaeogeothermal gradient in the preserved section is in the normal crustal range, then a straight-line projection of the palaeogeothermal gradient to an appropriate palaeo-surface temperature value will provide a reasonable estimate of the amount of eroded section (Fig. 3A; Yamaji, 1986; Schegg and Leu, 1998; Frings *et al.,* 2004). This procedure contains the implicit assumptions that the lithologies in the removed section were similar to those in the preserved section (i.e., large thicknesses of lithologies with extremes of thermal conductivity, e.g., salt or coal, were not formerly present) and, importantly, that the only source of heat was the basal heat-flow. The latter assumption is critical in regions, where fluid flow might be expected and may be the prime reason for grossly inaccurate erosion estimates, as discussed further below. The influence of advective heat transfer might be inferred for any basin that displays the following features (Ziagos and Blackwell, 1986; Lampe *et al.,* 2001; Green and

Fig. 3. Vitrinite reflectance (VR) data versus depth. **A.** Hypothetical example showing time-independent estimation of exhumed rocks. The VR values plotted on a logarithmic scale allow estimating thermal maturity gradient and the maximum thickness of the overburden (Yamaji, 1986; Connolly, 1989; Frings *et al.*, 2004). Assuming the palaeo-surface vitrinite (huminite) reflectance at c. 0.25%VR, the intersection of the regression line at this point can be used to predict the maximum overburden. Here, post-Cretaceous exhumation/erosion is c. 3,300 m. The regression line of the analysed VR measurements is extended to the value of 0.25% VR, which is the equivalent of a surface temperature of approximately 25°C. **B.** VR versus depth in the Opoczno PIG-2 well. Crosses means measured mean of VR value. Colour is adjusted from stratigraphy. Red dotted line means unconformity – in this case between lower Carboniferous and Zechstein. Note the rapid VR increase in Lower Triassic and decrease in Zechstein strata into sub-vertical profile. Non-linear VR profile suggest post-Early Triassic fluid flow influence on the Mesozoic profile. There is also VR jump at unconformity between Zechstein (1.37%) and lower Carboniferous (2.44%). Therefore, Carboniferous heat flow or/and burial were much higher than present-day. Lack of a longer VR profile in Carboniferous did not allow fixing any gradient, and further interpretation. Lower Carboniferous: upper Tournaisian to lower Visean. VR data from Swadowska (2006a) except of Jurassic VR from Grotek (2018).

Duddy, 2012): (1) palaeotemperatures are much higher than those predicted by the burial history under conditions of vertical conductive heat transfer; (2) palaeotemperature profiles fluctuate markedly, suggesting fluid-driven heat transfer along certain horizons; and (3) discrepancies between palaeotemperatures are derived from fluid inclusions, illite/smectite studies and kinetically dependent thermal maturity indicators, such as VR and/or apatite fission track data. Further information on this approach can be found in Duddy *et al.* (1994), Frings *et al.* (2004), and Botor (2012).

The basic geological data for thermal maturity analysis were taken from the following published monograph series: PGI Deep Boreholes Profiles – Opoczno PIG-2 (Kowalczewski, 2006a), Ostałów PIG-2 (Kowalczewski, 2006b), Nieświń PIG-1 (Fijałkowska-Mader, 2018), and Radwanów IG-1 (Jurkiewicz, 1980). VR data for these wells came from Swadowska (2006a, b) and Grotek (2018). Additionally, for the Radwanów IG-1 well, VR data from Grotek (2018) and Łuszczak *et al.* (2020) were used.

RESULTS AND INTERPRETATION

In the first step, the VR values were plotted on a logarithmic scale, which allowed an estimate of thermal maturity gradient and the maximum thickness of the eroded overburden (Yamaji, 1986; Connolly, 1989; Frings *et al.,* 2004). Assuming that the palaeosurface vitrinite (huminite) reflectance was c. 0.25% VR (equivalent to a palaeosurface temperature of c. 25 °C), the intersection of the regression line at this point can be used to predict the maximum eroded overburden (Fig. 3A). In the following step, VR values were used as an input parameter for the estimation of maximum palaeotemperature, after the Barker and Pawlewicz (1994) approach. By plotting these calculated temperatures against depth, palaeogeothermal gradients for the time of the highest temperatures in the basin can also be calculated. These calculations are based on the assumption that the thermal conductivity of the exhumed rocks was the same as that of those preserved in the analysed section (Yamaji, 1986; Connolly, 1989; Duddy *et al.,* 1994; Frings *et al.,* 2004; Green and Duddy, 2012). Thermal maturity trends were analysed by applying such an approach to four boreholes in the study area.

Opoczno PIG-2

In the Opoczno PIG-2 well, the VR dataset includes 10 samples from the Jurassic to the lower Carboniferous (Swadowska, 2006a; Grotek, 2018). The VR versus depth plot in the Opoczno PIG-2 well section shows a rapid VR increase from 0.48% (in the Jurassic) to 1.60% (in the Lower Triassic) and a decrease in the Zechstein strata (to 1.3% VR), forming an almost sub-vertical profile (Fig. 3B). Such a non-linear VR profile suggests a post-Early Triassic fluid flow influence on the Mesozoic profile. There is also a VR jump at the unconformity between the Zechstein Series (1.37%) and lower Carboniferous (2.44%). Therefore, pre-Permian heat flow and/or burial caused significant maturation of the Carboniferous organic matter, but the lack of longer VR profiles in the Carboniferous did not allow any gradient to be fixed or further interpretation to be carried out (Fig. 3B). A comparison of the present-day temperature profile (with a geothermal gradient of 22.5 °C/km) with both Mesozoic burial-induced (64 °C/km) and/or hydrothermally induced (96 °C/km) profiles in the Opoczno PIG-2 well shows that palaeotemperatures were higher in the past (Fig. 4). Both palaeogeothermal gradient values are very high. Therefore, the only plausible explanation is a fluid flow event.

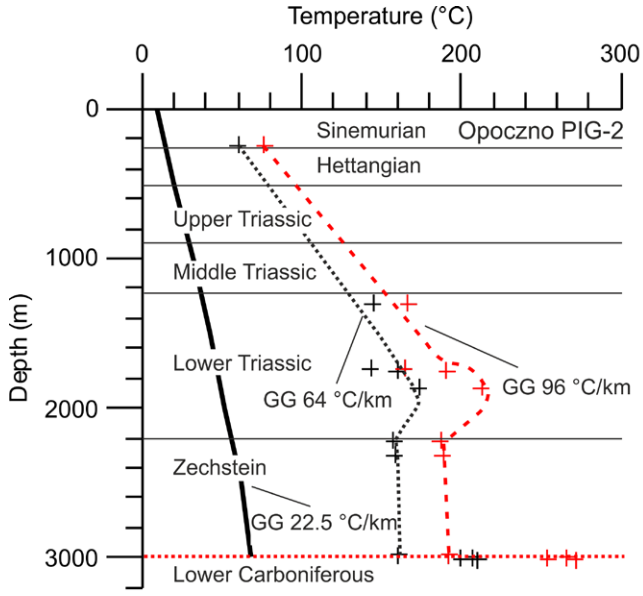

Fig. 4. Temperature profile in the Opoczno PIG-2 well. The bold black line (first from left) is the present-day temperature profile with a geothermal gradient (GG) of 22.5 °C/km. The black dotted curve is burial-related Tmax and the red dashed line is hydrothermal-related Tmax (both calculated from VR using the approach in Barker and Pawlewicz (1994). The horizontal red dotted line is an unconformity between the Carboniferous and the Zechstein. For other explanations, see Figure 3. Mesozoic palaeogeothermal gradient is extremely high (64–96 °C/km).

Ostałów PIG-2

The vitrinite reflectance versus depth plot in the Ostałów PIG-2 well shows that it is not possible to achieve a single VR gradient (Swadowska, 2006b). The Middle Triassic value (0.83% VR) follows a decrease in the Zechstein strata (0.74–0.78%), into a sub-vertical profile. The change in VR from the Zechstein to the Triassic is not significant, but it causes a non-linear VR profile to occur and suggests the influence of post-Early Triassic fluid flow on the Mesozoic profile. There is also a significant jump in VR at the unconformity between the Permian (0.74%) and the lower Carboniferous (1.60%). Therefore, Carboniferous heat flow and/or burial were much higher than at present. The VR profile in the Carboniferous is short; however, it suggests c. 3 km of pre-Permian exhumation. This value can be accepted because Mesozoic fluid temperatures seem to be much lower; this was not an overprinted Variscan signal (Fig. 5). In the Ostałów PIG-2 well, there was a linear increase in present-day

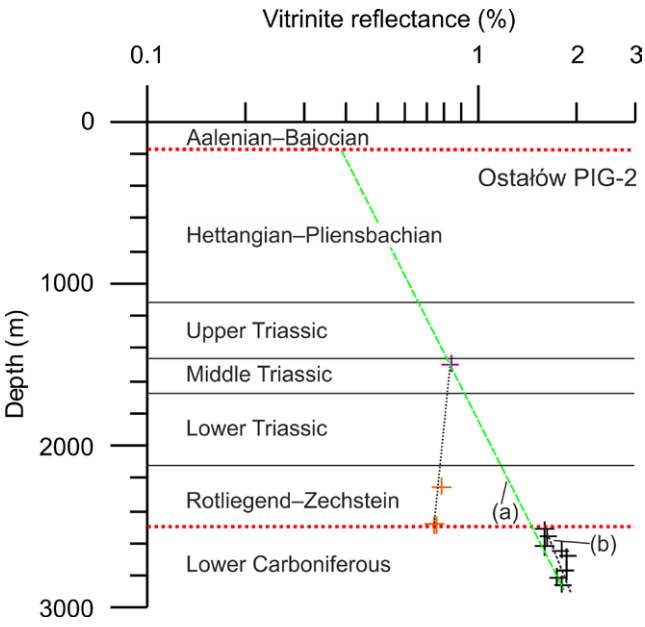

Fig. 5. Vitrinite reflectance versus depth in the Ostałów PIG-2 well. It is not possible to achieve a single VR gradient (green curve - a). The Middle Triassic value (0.83% VR) is following the decrease in Zechstein strata (0.74–0.78%) into the sub-vertical profile. The change in VR from Triassic to Zechstein is not significant but it causes the non-linear VR profile to occur, suggesting a post-Early Triassic fluid flow influence on the Mesozoic profile. There is also a VR jump at the unconformity between the Permian (0.74%) and lower Carboniferous (1.60%). The VR profile in the Carboniferous section is short (black - b); however, it suggests c. 3 km pre-Permian exhumation. For other explanations see Figure 3.

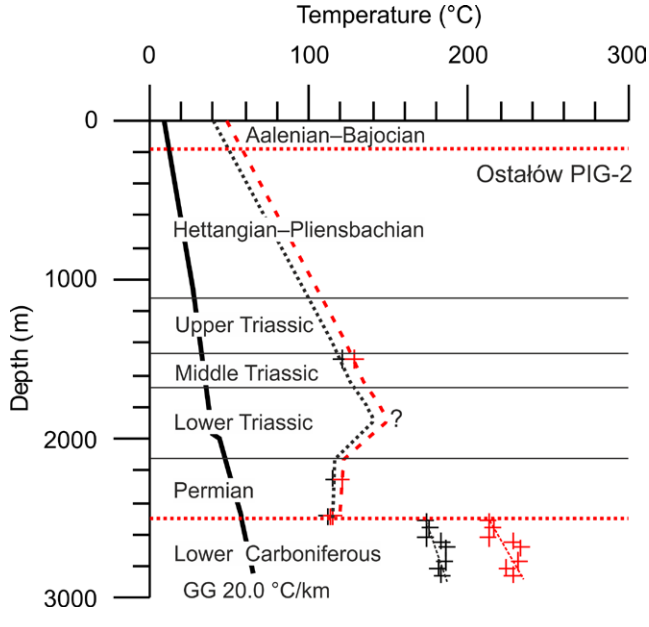

Fig. 6. Temperature profile in the Ostałów PIG-2 well. The bold black line (first from left) is the present-day temperature. The black dotted curve is burial-related Tmax and the red ones are hydrothermal-related Tmax (both calculated from VR using the approach in Barker and Pawlewicz (1994). Both curves are interpretations, as only crosses are based on VR measurements. All curves show that it was hotter in the past than the present day. Palaeogeothermal gradients were different in the Permian–Mesozoic and Carboniferous. GG – geothermal gradient. For other explanations see Figure 3.

temperature, showing a geothermal gradient of 20 °C/km; whereas the palaeotemperature profile calculated from VR data is non-linear (Fig. 6). Palaeotemperatures show that it was hotter in the past than at present. Palaeogeothermal gradients were different in the Permian–Mesozoic and in the Carboniferous. However, in the Triassic–Jurassic section there is only 1 VR value, which prevents the fixing of a palaeogeothermal gradient. The Carboniferous section is short (c. 300 m), showing a palaeogeothermal gradient of 33 °C/km (for the burial-induced model) or c. 60 °C/km (for the hydrothermal-induced model; Fig. 6).

Nieświń PIG-1

In the Nieświń PIG-1 well, the oldest documented strata are sandstones and siltstones of the lower Carboniferous, which were not entirely drilled and, moreover, they have been strongly folded and faulted, as demonstrated by the repetition of the sequence between the Zechstein layers and the Carboniferous. The thermal maturity data in Grotek (2018) gave VR values for the Lower Jurassic (Hettangian) to lower Carboniferous section in the Nieświń PIG-1 well. The 18 values ranged from 0.56–1.73% VR (Fig. 7). In most samples, 20 to 82 organic particles were measured per single sample. The range of measurements in each sample showed some variation; however, standard deviations were not given (Grotek, 2018). Nevertheless, it seems that the entire VR

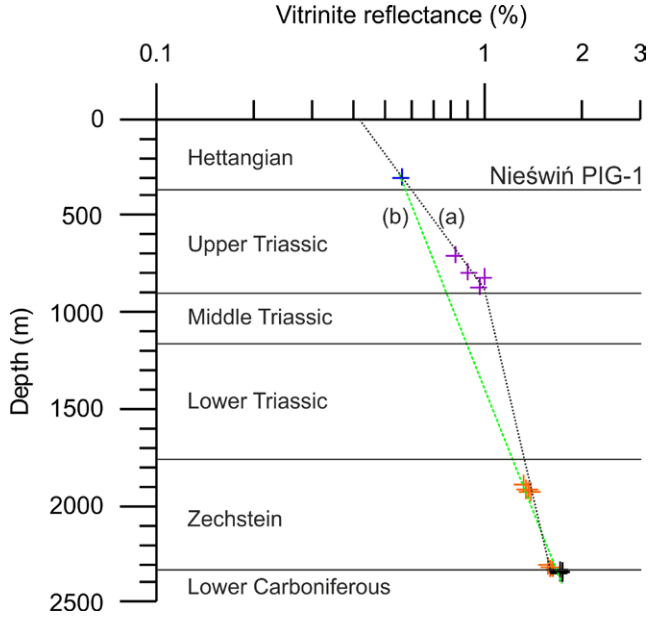

Fig. 7. VR versus depth in the Nieświń PIG-1 well. There is no uniform VR gradient. The Upper Triassic samples show particularly elevated VR values. At least two VR gradients (a and b) can occur in the Mesozoic profile, showing 500 m (a) or 1,900 m (b) post-Hettangian exhumation, respectively. At the unconformity between the Zechstein and the lower Carboniferous, no thermal maturity breaks exist. However, due to the strata repetition, caused by a fault in the bottom part of the well section, the Zechstein and lower Carboniferous strata are tectonically disturbed. Unfortunately, the Carboniferous part of the section is too short to fix any gradient. For other explanations see Figure 3.

profile shows consistent data results, with $R^2 = 0.96$. VR increases systematically with depth. However, more detailed study shows that there are at least two gradients, instead of one. The break between them is within the continuous sedimentary section of the Middle Triassic. Therefore, this excludes any exhumation manifested by unconformities but might indicate the influence of fluid flow heating. Unfortunately, there are no VR data in the deeper part of the profile, i.e., within the Lower Triassic, which is dominated by sandstones. The Permian to Hettangian VR trend shows c. 1900 m exhumation, which could have been c. 500 m, if only the Upper Triassic-Hettangian data are considered (Fig. 7). Another interesting feature is the lack of a break in the VR profile between the Zechstein and the Carboniferous, where there is a significant time gap in the geological record. VR values of ca. 1.7% occur above (Zechstein) and below (Carboniferous) this unconformity (Grotek, 2018). The calculated Mesozoic palaeogeothermal gradient in the Nieświń PIG-1 borehole is 45 °C/km, in the burial model, and 70 °C/km, in the hydrothermal model (Fig. 8).

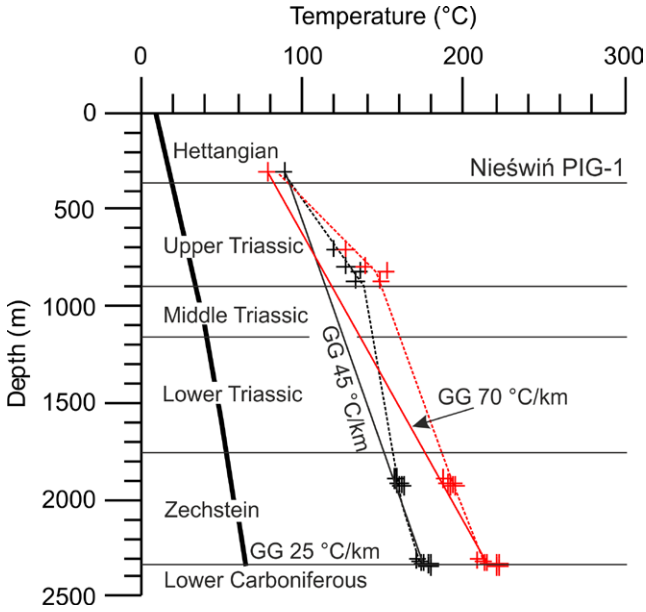

Fig. 8. Temperature profile in the Nieświń PIG-1 well. The bold black line (first from left) is the present-day temperature. Present-day geothermal gradient is 25 ºC/km. In the analysed well section, at least two palaeogeothermal gradients occurs within the Mesozoic. The black dotted curve is the burial-related Tmax trend, and the red ones are the hydrothermal-related Tmax trend (both calculated from VR, using the approach in Barker and Pawlewicz (1994). Palaeogeothermal gradient for burial Tmax values is 45 °C/km (black solid line). Palaeogeothermal gradient for hydrothermal Tmax is 70 °C/km (red solid line). For other explanations see Figure 3.

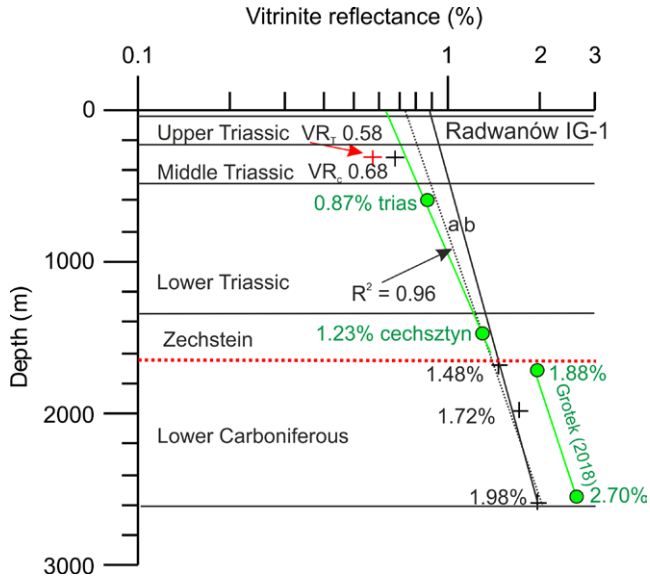

Fig. 9. VR profile in the Radwanów IG-1 well. Carboniferous VR values (black crosses) are taken from Łuszczak *et al.* (2020). The stratigraphy is from Jurkiewicz (1980). Green values are from Grotek (2018). Triassic VR values (black and red crosses) are estimated from surface biomarker data (Kolonia Jakimowska, Marynowski *et al.,* 2002). VRT is from the terphenyl parameter, VRc is from methylophenantrene (Rc[%] = 0.60 MPI1 + 0.40 for VR<1.35%) (Radke and Welte, 1983). MPI1 — methylphenanthrene index 1-MPI1 = 1.5([2-MP] + [3-MP])/([P] + [1-MP] + [9-MP]) (Radke and Welte, 1983). The exact depth of the Triassic samples and Grotek`s (2018) samples is roughly estimated. Grotek's (2018) data show a significant shift of VR gradient between the Zechstein (1.23% VR) and the Carboniferous (1.88% VR). The average Carboniferous–Triassic VR gradient appears to be uniform ('a' curve, $R^2 = 0.96$), suggesting 1800 m exhumation of post-Triassic sediments, which is also confirmed by the Permian–Triassic VR data from Grotek (2018). The Carboniferous VR gradient ('b' curve) shows estimated exhumation to be c. 5 km. Carboniferous VR data from Grotek (2018) also suggest similar exhumation. For other explanations see Figure 3.

Radwanów IG-1

The VR data for Radwanów IG-1 are not uniform (Fig. 9). Triassic thermal maturity was estimated by Łuszczak *et al.* (2020) from surface biomarker data from the Kolonia Jakimowska outcrop, for which the calculated VR is c. 0.6% (Marynowski *et al.,* 2002). Moreover, Grotek`s (2018) VR data show a significant shift of VR values between the Zechstein (1.23% VR) and the Carboniferous (1.88–2.70% VR). Unfortunately, there is no depth given in Grotek`s (2018) work for this well because VR values are only given in a map of the study area. Large discrepancies exist between the Łuszczak *et al*. (2020) and Grotek (2018) VR data. The latter seem to be more reliable, as they show the same dog-leg pattern (or 'jump') at the Carboniferous-Permian boundary, as is the case elsewhere in the region. Moreover, the Łuszczak *et al*. (2020) data were not measured VR values but were re-calculated from biomarker data, which are not very precise. Nevertheless, the VR values show a thermal maturity jump across the unconformity between the Permian and the lower Carboniferous (Fig. 9). However, the average Carboniferous–Triassic VR gradient appears to be uniform ('a' curve, $R^2 = 0.96$), suggesting 1,800 m exhumation of post-Triassic sediments, which also was confirmed by the Permian-Triassic VR data from Grotek (2018). Applying only the Carboniferous section VR gradient ('b' curve) gives

an estimated exhumation of c. 5 km. Carboniferous VR data from Grotek (2018) suggest similar exhumation. Moreover, the VR jump between the Permian and Carboniferous strata is clear in the adjacent wells in the area NE of the HCM (Grotek, 2018). For example, in Łopuszno IG-1, the VR is 0.83% in the Permian and 2.55 % in the Carboniferous. The linear present-day temperature profile for the Radwanów IG-1 well shows a geothermal gradient of 30.5 °C/km (Fig. 10). All VR-derived paleotemperatures using Barker and Pawlewicz (1994) show that it was much hotter in the past. The burial-related palaeogeothermal gradient is 32 °C/km and the hydrothermal-related gradient is 43 °C/km, from the VR data in Łuszczak *et al.* (2020). The palaeogeothermal gradient calculated from Grotek's data ('c' and 'd' curves) show a break at the unconformity between the Permian and the Carboniferous. Assuming a hydrothermal model or burial model for the Carboniferous section only, c. 4 km and 5 km of Carboniferous overburden were removed, respectively.

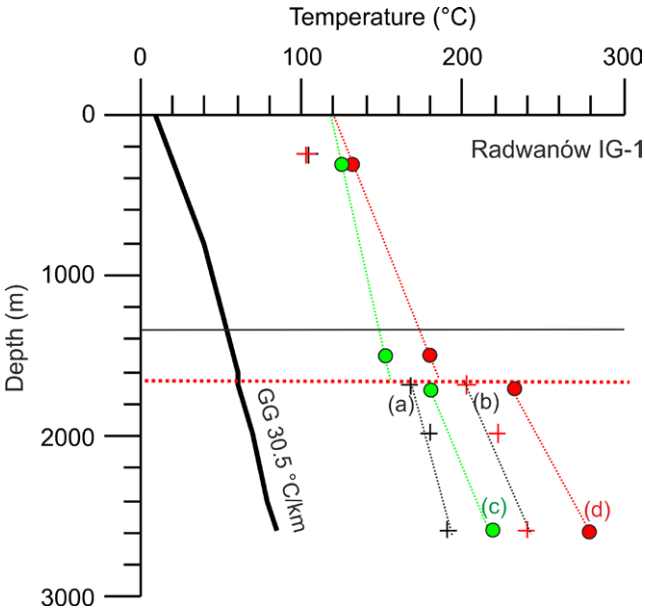

Fig. 10. Temperature profile for the Radwanów IG-1 well. The bold black line (first from left) is the present-day temperature profile with a geothermal gradient (GG) of 30.5 °C/km. The VR-derived palaeotemperature (black and red crosses) are from Łuszczak *et al.* (2020). The VR-derived palaeotemperature (green and red dots) are from Grotek (2018). All palaeotemperatures were calculated from VR, using Barker and Pawlewicz (1994). The black dotted curve (a) is burial-related Tmax (palaeogeothermal gradient 32 °C/km) and the red ones (b) are hydrothermal-related Tmax (43 °C/km) from the VR data of Łuszczak *et al.* (2020). The palaeogeothermal gradient calculated from Grotek data ('c' and 'd' curves) show a break at the unconformity between the Permian and the Carboniferous. The stratigraphy and present-day temperature profile are from Jurkiewicz (1980). For other explanations see Figure 3. The lower Carboniferous comprises upper Tournaisian to lower Viséan strata. Assuming a hydrothermal model or burial model, c. 4 km or 5 km of Carboniferous overburden were exhumed. Further explanations are given in the text.

DISCUSSION

Plots of VR against depth (Figs 3–10) exhibit several trends in the analysed wells. First of all, the palaeotemperatures calculated from VR data show that it was much hotter in the past than at the present-day. One of the most prominent features of thermal evolution, recognised in these wells, is that Mesozoic fluid flow caused overprinting of the burial-induced diagenetic effects. The shape of the VR curves in the borehole sections allows the suggestion that fluid flow occurred. In particular, the non-linear VR profiles (sensu Ziagos and Blackwell, 1986) above the Permian/Carboniferous unconformity (in Triassic strata), show that fluid flow may have contributed to the maturation of the organic matter contained in Mesozoic sediments (Figs 3–8). Owing to the post-Triassic fluid flow event, an assessment of post-Triassic exhumation might be overestimated and it is not attempted here. Moreover, in the Lower Triassic sandstones in the Opoczno PIG-2 and Nieświń PIG-1 boreholes, some hydrothermal copper mineralization appears (Kowalczewski, 2006a, b), suggesting the occurrence of fluid flow. The most likely mechanism responsible for a non-linear VR pattern in Triassic rocks is lateral fluid flow that developed regionally during the Jurassic period (Kozłowska and Poprawa, 2004; Poprawa *et al.,* 2005; Kuberska *et al.,* 2021). However, the Ar-Ar ages for the Wzorki diabase in the Łysogóry Unit showed that the strong hydrothermal alteration took place in the Middle Triassic (Nawrocki *et al.,* 2013). Lateral variations in the palaeogeothermal gradients, recorded in the Permian-Mesozoic sections between wells, are consistent with a gravity-driven hydrothermal system, discharging heated fluids along fault systems. Palaeogeothermal gradients are substantially higher in the Carboniferous sections (mean 60 °C/km) than in the Mesozoic sections (mean 32 °C/km). Thermal maturity in the Carboniferous sections is considered to be the consequence of burial, elevated heat flow and a regional advective system during the late Carboniferous to early Permian, rather than Mesozoic or Cenozoic processes. In most of the analysed well sections, positive VR anomalies occur against the general trend of thermal maturity, increasing with depth (Figs 3, 7, 8). Unfortunately, the analysed wells did not have the suitably long VR sections, required for detailed recognition of the Carboniferous thermal regime pattern. The sources of the heat in the late Carboniferous to early Permian can be related to well-known magmatism and hydrothermal processes along TTZ (Narkiewicz *et al.*, 2010; Nawrocki *et al.,* 2013; Krzemińska and Krzemiński, 2019). Moreover, the regionally distributed low thermal maturity data (usually below 0.5% VR) in Mesozoic sediments in the HCM and adjacent areas, are against an increase in the thermal maturity of Palaeozoic rocks after the Permian (Marynowski *et al.,* 2002; Narkiewicz and Malec, 2005). Therefore, different thermal events governed Palaeozoic and Mesozoic thermal regimes.

The results partly agree with the thermal maturity modelling results in Poprawa *et al*. (2005), who showed that thermal maturity depth profiles in the Mesozoic successions of the southwest of the HCM allow the reconstruction of the Late Jurassic phase of hot fluid migration, presumably

related to the enhanced permeability of the faults and fractures driven by extension. Poprawa *et al.* (2005) assumed two discrete phases of fluid circulation: in the late Carboniferous to early Permian and, more importantly, in the Late Jurassic. However, in the analysed well sections, VR pattern breaks at the base of the Permian unconformity exclude the occurrence of a single late Mesozoic thermal event. Moreover, zircon helium ages of Ordovician to lower Carboniferous samples show that a distinct cooling event occurred in the transition from the late Carboniferous to the early Permian (Botor *et al.,* 2018). Additionally, in the SW part of the HCM, Kowala and Ostrówka bentonite samples show apatite fission tracks, documenting only slow cooling through the entire Mesozoic and Cenozoic. These samples have zircon helium ages of c. 300 Ma and probably show that the maximum heating should have occurred in the middle of the Carboniferous (Fig. 2; Botor *et al.,* 2018). In the Kowala section, the immature character of the organic matter indicates maximum burial temperatures lower than c. 80 °C, based on CAI (Bełka, 1990). Very low maturity is also confirmed by an average vitrinite reflectance value of 0.53% VR (Marynowski *et al.,* 2001). However, on the basis of smectite illitization, the temperature was estimated at c. 120–140 ºC (Środoń and Trela, 2012). Therefore, there is a significant discrepancy between the maximum temperatures, estimated from organic and mineral indices. Since the ZHe ages for a bentonite horizon from the Kowala section were reset, this was considered to be evidence of local, at least short-term, hydrothermal fluid flow, which did not change the thermal maturity of organic matter but influenced the mineral record in these rocks (Botor *et al.,* 2018). The maturation of organic matter requires a longer time than the annealing of an AFT thermochronometer. A minimum of 10^6–10^7 years of continuous heating is usually necessary to stabilize thermal maturation (Barker, 1989), whereas, annealing of fission tracks in apatite requires much less time (Crowley *et al.,* 1991). The age of diagenesis of clay minerals was documented by illite K-Ar dates from the Kowala section by Zwing (2003) and found to be in the range 315–292 Ma. Środoń and Trela (2012) published illite K-Ar ages in the range 192–228 Ma.

Fluid circulation can cause an increase in heat flow at shallow levels in a short time, by a factor of five over the basement heat flow (Gayer *et al.,* 1998a, b). However, any approach based on conductive heat transfer (e.g., thermal maturity modelling by PetroMod software) cannot detect such short-lived convection processes in the crust. Nevertheless, this does not contradict their existence. Therefore, the concept of high heat flow does not contradict an occurrence of fluid flow events. In fact, high heat flow, related to extensional processes along faults, could trigger fluid flow circulation, which has been shown in many papers (e.g., Duddy *et al.,* 1994; Frey and Robinson, 1999; Lampe *et al.,* 2001). Analysis of a number of samples over a depth range yields information about the palaeotemperature profile with depth. Heating because of continuous burial, in conditions that give rise to a constant geothermal gradient, should produce a linear profile, the gradient of which reflects the palaeogeothermal gradient at the maximum burial in the basin history. Conversely, a fluctuating palaeotemperature profile indicates localised heating by igneous intrusions (Summer and Verosub, 1992) and/or the input from anomalously hot fluids along certain horizons (Ziagos and Blackwell, 1986; Duddy *et al.,* 1994). In a study of the Rhine graben, Person and Garven (1992) modelled the influence of heated fluids on hydrocarbon source-rock maturation patterns and concluded that a topographically driven fluid flow system could properly explain the present-day heat flow data and the measured thermal maturation data. Summer and Verosub (1992) showed the thermal effects, related to fluid flow in strata below volcanic sequences in Oregon. They recognized the importance of vertical thermal maturity sections in the interpretation of a fluid flow mechanism for heating and the mistakes in overburden estimation that would result if lateral heat transfer was not recognized. Differences in vitrinite reflectance profiles have also been recorded between ground-water recharge and discharge areas in the Uinta basin, by Willett and Chapman (1987).

Apatite helium and fission track data from the northern margin of the Palaeozoic core show rather slow cooling in the Mesozoic-Cenozoic (Cattò, 2014). Therefore, it seems that, farther from the HCF, thermochronology data do not show a significant or rapid cooling record due to tectonic inversion in the Late Cretaceous to early Palaeogene, in contrast to data close to the HCF (Botor *et al.,* 2018; Łuszczak *et al.,* 2020).

Cooling due to tectonic inversion in the HCM and adjacent areas of the Mid-Polish Trough (Fig. 2) was recently documented by thermochronology data (Botor *et al.,* 2018; Łuszczak *et al.,* 2020). This cooling had already started in the late Cenomanian to early Campanian (Fig. 2; c. 100–90 Ma, Łysogóry) and c. 90 Ma in the Kielce Unit (Botor *et al.,* 2018), as well c. 91–82 Ma in the Radwanów IG-1 section (Łuszczak *et al.,* 2020). The late Turonian to early Campanian (c. 80–90 Ma) onset of tectonic inversion is also similar to that in the Intra-Sudetic Basin (Botor *et al.,* 2019; Sobczyk *et al.,* 2020). The seismic investigation results along the Mid-Polish Trough also suggest similar timing for the onset of tectonic inversion (Krzywiec *et al.,* 2009, 2018). Such timing of tectonic inversion was interpreted by Resak *et al*. (2008, 2010) and Narkiewicz *et al*. (2010), who also provided a comparison with the German Basin. This timing of the inversion is almost identical with the start of the inversion of Mesozoic basins, such as the Lower Saxony Basin farther west, in Germany (Mazur *et al.*, 2005; Senglaub *et al.,* 2005). The above-mentioned data show that, in the Late Cretaceous (and definitely before the Maastrichtian), the crust in Central Europe was deformed in a compressive to transpressional regime (Kley and Voigt, 2008). This caused the reactivation of Variscan faults, the exhumation of tectonic blocks and, finally, the inversion of the Cretaceous basins (Lamarche *et al.*, 2003b). Comprehensive analysis of apatite fission tracks, zircon helium ages and the thermal maturity of organic matter in the area NE of the TTZ (East European Platform) showed that a major heating of Palaeozoic strata (up to the Carboniferous, inclusive) occurred before the Permian, reaching maximum temperatures in the early and late Carboniferous in the Baltic-Podlasie Basin and the Lublin Basin, respectively (Botor *et al.,* 2021). The borehole sections analysed here are

located in the area of the northern Permian-Mesozoic margin of the HCM that is within the south-eastern part of the Mid-Polish Swell. Therefore, it appears that major factors, influencing the thermal history of these rocks, were burial in the Mesozoic, causing heating, and the Late Cretaceous to early Palaeogene tectonic inversion, causing cooling. However, fluid flow events also contributed to the thermal history of this area.

CONCLUSIONS

VR analysis was applied to borehole sections to establish the burial and thermal evolution of the northern margin of the HCM. In the majority of the sections, a VR break occurs at the base of the Permian, which proves the development of Variscan thermal maturity taking place in conditions different from those in the Mesozoic.

Thermal maturity of the Carboniferous strata was reached at the end of the late Carboniferous and was not overprinted by any Mesozoic processes. The influence of Permian–Mesozoic burial on the thermal maturity of Carboniferous and, by implication, older strata was limited. Both sedimentary burial and hydrothermal processes could have contributed to a high level of thermal maturation of these Carboniferous rocks.

Calculated palaeogeothermal gradients, based on VR data, reaching up to 96 ºC/km (probably in the Jurassic), strongly suggest the influence of fluid flow. Considering the tectonic development of the study area, such high gradients cannot be explained purely by changes in the basal heat flow. The non-linear VR pattern in the Permian-Triassic strata suggests that it was caused by hot fluid flow in the Jurassic.

Acknowledgments

This work was supported by AGH Statutory Research Project No. 16.16.140.315. I would like to thank Marek Narkiewicz (Warsaw, Poland) and Silvia Omodeo Salé (University of Geneva, Switzerland), as well as the journal editors, for their insightful comments.

REFERENCES

Akande, S. O. & Erdtmann, B. D., 1998. Burial metamorphism (thermal maturation) in Cretaceous sediments of the Southern Benue Trough and Anambra Basin, Nigeria. *AAPG Bulletin*, 82: 1191–1206.

Barker, C. E., 1983. Influence of time on metamorphism of sedimentary organic matter in liquid-dominated geothermal systems, western North America. *Geology,* 11: 384–388.

Barker, C. E., 1989. Temperature and time in the thermal maturation of sedimentary organic matter. In: Naeser, N. D. & McCulloh, T. H. (eds), *Thermal history of sedimentary basins*. Springer, Heidelberg, pp. 73–98.

Barker, C. E. & Goldstein, R. H., 1990. Fluid–inclusion technique for determining maximum temperature in calcite and its comparison to the vitrinite reflectance geothermometer. *Geology,* 18: 1003–1006.

Barker, C. E. & Pawlewicz, M. J., 1994. Calculation of vitrinite reflectance from thermal histories and peak temperatures. A comparison of methods. In: Mukhopadhyay, P. K. & Dow, W. G. (eds), *Vitrinite reflectance as a maturity parameter: applications and limitations*. *ACS Symposium Series,* 570: 216–229.

Bełka, Z., 1990. Thermal maturation and burial history from conodont colour alteration data, Holy Cross Mountains, Poland. *Courier Forschungsinstitut Senckenberg*, 118: 241–251.

Bełka, Z. & Siewniak-Madej, A., 1996. Thermal maturation of the Lower Paleozoic strata in the southwestern margin of the Małopolska Massif, southern Poland: no evidence for Caledonian regional metamorphism. *Geologische Rundschau*, 85: 775–781.

Botor, D., 2012. Hydrothermal fluid influence on the thermal evolution of the Stephanian sequence of the Sabero Coalfield (NW Spain). *Geology, Geophysics & Environment*, 38: 369–393.

Botor, D., Anczkiewicz, A., Dunkl, I., Golonka, J., Paszkowski, M. & Mazur, S., 2018. Tectonothermal history of the Holy Cross Mountains (Poland) in the light of low-temperature thermochronology. *Terra Nova,* 30: 270–278.

Botor, D., Anczkiewicz, A., Mazur, S. & Siwecki, T., 2019. Post-Variscan thermal history of the Intra-Sudetic Basin (Sudetes, Bohemian Massif) based on apatite fission track analyzis. *International Journal of Earth Sciences,* 108: 2561–2576.

Botor, D., Mazur, S., Anczkiewicz, A., Dunkl, I. & Golonka, J., 2021. Thermal history of the East European Platform margin in Poland based on apatite and zircon low-temperature thermochronology. *Solid Earth,* 12: 1899–1930.

Cattò, S., 2014. *Tectonic evolution of the Holy Cross Mountains (Poland)*. Unpublished Ph.D. Thesis, Padua University, 103 pp.

Cavailhes, T., Rotevatn, A., Monstad, S., Khala, A. B., Funk, E., Canner, K., Looser, M., Chalabi, A., Gay, A., Travé, A., Ferhi, F., Skanji, A., Chebbi, R. M. & Bang, N., 2018. Basin tectonic history and paleo-physiography of the pelagian platform, northern Tunisia, using vitrinite reflectance data. *Basin Research*, 30: 926–941.

Connolly, C. A., 1989. Thermal history and diagenesis of the Wilrich Member shale, Spirit River Formation, northwest Alberta. *Canadian Petroleum Geology Bulletin,* 37: 182–197.

Crowley, K., Cameron, M. & Schaefer, R. L., 1991. Experimental studies of annealing of etched fission tracks in fluorite. *Geochimica et Cosmochimica Acta*, 55: 1449–1465.

Dadlez, R., Kowalczewski, Z. & Znosko, J., 1994. Some key problems of the pre-Permian tectonics of Poland. *Geological Quarterly*, 38: 169–190.

Dadlez, R., Marek, S. & Pokorski, J., 2000. *Geological map of Poland without Cenozoic deposits, scale 1:1 000 000*. Państwowy Instytut Geologiczny, Warsaw.

Dadlez, R., Narkiewicz, M., Stephenson, R. A., Visser, M. T. M. & Van Wees, J. D., 1995. Tectonic evolution of the Mid-Polish Trough: modeling implications and significance for central European geology. *Tectonophysics,* 252: 179–195.

Dalla Torre, M., Ferreiro Mählmann, R. & Ernst, W. G., 1997. Experimental study on the pressure dependence of vitrinite maturation. *Geochimica et Cosmochimica Acta,* 61: 2921–2928.

Duddy, I. R., Green, P. F., Bray, R. J. & Hegarty, K. A., 1994. Recognition of the thermal effects of fluid flow in sedimentary

basins. In: Parnell, J. (ed.), *Geofluids: Origin, Migration and Evolution of Fluids in Sedimentary Basins*. *Geological Society, London, Special Publications*, 78: 325–345.

Fijałkowska-Mader, A. (ed.), 2018. Nieświń PIG-1. *Profile głębokich otworów wiertniczych Państwowego Instytutu Geologicznego*, 151: 1–215. [In Polish.]

Frey, M. & Robinson, D., 1999. *Low-Grade Metamorphism*. Blackwell Science, Cambridge, 313 pp.

Frings, U., Lutz, R., de Wall, H. & Warr, L. N., 2004. Coalification history of the Cinera-Matallana pull-apart basin (NW Spain). *International Journal of Earth Sciences*, 93: 92–106.

Gayer, R. A., Garven, G. & Rickard, D. T., 1998a. Fluid migration and coal-rank development in foreland basins. *Geology,* 26: 679– 682.

Gayer, R. A., Hathaway, T. M. & Nemčok, M., 1998b. Transpressionaly driven rotation in the external orogenic zones of the Western Carpathians and the SW British Variscides. In: Holdsworth, R. E., Strachan, R. A. & Dewey, J. F. (eds), *Continental Transpressional and Transtensional Tectonics*. *Geological Society of London, Special Publication*, 135: 235–266.

Green, P. F. & Duddy, I. R., 2012. Thermal history reconstruction in sedimentary basins using apatite fission-track analyzis and related techniques, analyzing the thermal history of sedimentary basins. In: Harris, N. B. & Peters, K. E. (eds), *Methods and Case Studies. SEPM Society for Sedimentary Geology*, 103: 65–104.

Grotek, I., 1998. Thermal maturity of organic matter in the Zechstein deposits of the Polish Lowlands area. *Prace Państwowego Instytutu Geologicznego*, 165: 255–259. [In Polish, with English summary.]

Grotek, I., 2018. Charakterystyka petrograficzna oraz dojrzałość termiczna materii organicznej rozproszonej w utworach karbonu–jury. In: Fijałkowska-Mader, A. (ed.), *Nieświń PIG-1. Profile głębokich otworów wiertniczych Państwowego Instytutu Geologicznego*, 151: 141–146. [In Polish, with English summary.]

Hakenberg, M. & Świdrowska, J., 1998. Evolution of the Holy Cross segment of the Mid-Polish Trough during the Cretaceous. *Geological Quarterly*, 42: 239–262.

Hantschel, T. & Kauerauf, A., 2009. *Fundamentals of Basin and Petroleum Systems Modeling*. Springer, Heidelberg, 607 pp.

Huang, W. L., 1996. Experimental study of vitrinite maturation: Effect of temperature, time, pressure, water, and hydrogen index. *Organic Geochemistry,* 24: 233–241.

Jarosiński, M., Poprawa, P. & Ziegler, P. A., 2009. Cenozoic dynamic evolution of the Polish Platform. *Geological Quarterly*, 53: 3–26.

Jaworowski, K., 2002. Geotectonic significance of Carboniferous deposits NW of the Holy Cross Mts. (central Poland). *Geological Quarterly,* 46: 267–280.

Jurkiewicz, H. (ed.), 1980. Radwanów IG-1. *Profile głębokich otworów wiertniczych Państwowego Instytutu Geologicznego.* Wydawnictwa Geologiczne, Warszawa, 113 pp. [In Polish.]

Kalvoda, J., Bábek, O., Fatka, J., Leichmann, R., Melichar, S., Nehyba, P. & Špaček, P., 2008. Brunovistulian terrane (Bohemian Massif, Central Europe) from Late Proterozoic to Late Paleozoic: a review. *International Journal of Earth Sciences,* 97: 497–518.

Ketcham, R. A., 2005. Forward and inverse modelling of low-temperature thermochronometry data. *Reviews in Mineralogy and Geochemistry*, 58: 275–314.

Kley, J. & Voigt, T., 2008. Late Cretaceous intraplate thrusting in central Europe: effect of Africa-Iberia-Europe convergence, not Alpine collision. *Geology,* 36: 839–842.

Konon, A., 2006. Buckle folding in the Kielce Unit, Holy Cross Mountains, central Poland. *Acta Geologica Polonica*, 56: 375–405.

Kowalczewski, Z., 2006a. Opoczno PIG-2. *Profile głębokich otworów wiertniczych Państwowego Instytutu Geologicznego*, 111: 1–139. [In Polish.]

Kowalczewski, Z., 2006b. Ostałów PIG-2. *Profile głębokich otworów wiertniczych Państwowego Instytutu Geologicznego,* 112: 1–133. [In Polish.]

Kozłowska, A. & Poprawa, P., 2004. Diagenesis of the Carboniferous clastic sediments of the Mazowsze region and the northern Lublin region related to their burial and thermal history. *Przegląd Geologiczny*, 52: 491–500. [In Polish, with English summary.]

Krzemińska, E. & Krzemiński, L., 2019. Magmatic episodes in the Holy Cross Mountains, Poland – a new contribution from multi-age zircon populations. *Biuletyn Państwowego Instytutu Geologicznego*, 474: 43–58.

Krzemiński, L., 1999. Anorogenic Carboniferous sandstones from the northwestern border of the Holy Cross Mountains, Central Poland. *Przegląd Geologiczny,* 47: 978–986. [In Polish, with English summary.]

Krzywiec, P., 2002. Mid-Polish Trough inversion – seismic examples, main mechanisms and its relationship to the Alpine-Carpathian collision. In: Berotti, G., Schulmann, K. & Cloetingh, S. (eds), *Continental Collision and the Tectonosedimentary Evolution of Forelands. European Geosciences Union, Stephan Mueller Special Publication Series*, 1: 151–165.

Krzywiec, P., 2009. Devonian–Cretaceous repeated subsidence and uplift along the Teisseyre-Tornquist zone in SE Poland – Insight from seismic data interpretation. *Tectonophysics*, 475: 142–159.

Krzywiec, P., Gągała, Ł., Mazur, S., Słonka, Ł., Kufrasa, M., Malinowski, M., Pietsch, K. & Golonka, J., 2017a. Variscan deformation along the Teisseyre-Tornquist Zone in SE Poland: Thick-skinned structural inheritance or thin-skinned thrusting? *Tectonophysics,* 718: 83–91.

Krzywiec, P., Gutowski, J., Walaszczyk, I., Wróbel, G. & Wybraniec, S., 2009. Tectonostratigraphic model of the Late Cretaceous inversion along the Nowe Miasto-Zawichost Fault Zone, SE Mid-Polish Trough. *Geological Quarterly*, 53: 27–48.

Krzywiec, P., Mazur, S., Gągała, Ł., Kufrasa, M., Lewandowski, M., Malinowski, M. & Buffenmyer, V., 2017b. Late Carboniferous thin-skinned compressional deformation above the SW edge of the East European craton as revealed by seismic reflection and potential field data – Correlations with the Variscides and the Appalachians. In: Law, R. D., Thigpen, J. R., Merschat, A. J. & Stowell, H. H. (eds), *Linkages and Feedbacks in Orogenic Systems*. *Geological Society of America Memoir,* 213: 353–372.

Krzywiec, P., Stachowska, A. & Stypa, A., 2018. The only way is up–on Mesozoic uplifts and basin inversion events in SE

Poland. *Geological Society of London Special Publications,* 469: 33–57.

Kuberska, M., Kiersnowski, H., Poprawa, P. & Kozłowska, A., 2021. Rotliegend sedimentary rocks in the Kutno-2 well under conditions of a postulated Jurassic thermal event and high overpressure – a petrographic study. *Przegląd Geologiczny*, 69: 365–373. [In Polish, with English abstract.]

Kuleta, M. & Zbroja, S., 2006. Wczesny etap rozwoju pokrywy permsko-mezozoicznej w Górach Świętokrzyskich. In: Skompski, S. & Żylińska, A. (eds), *77 Zjazd Naukowy Polskiego Towarzystwa Geologicznego, Ameliówka k. Kielc, 28–30 czerwca 2006 r., Materiały konferencyjne*, Wydawnictwo Państwowego Instytutu Geologicznego, Warszawa, pp. 105–125. [In Polish.]

Kutek, J., 1968. The Kimmeridgian and Uppermost Oxfordian in the SW margin of the Holy Cross Mountains, Central Poland. Part I. Stratigraphy. *Acta Geologica Polonica*, 18: 493–586. [In Polish, with English summary.]

Kutek, J., 2001. The Polish Permo-Mesozoic Rift Basin. *Mémoires du Muséum national d'histoire naturelle*, 186*:* 213–236.

Kutek, J. & Głazek, J., 1972. The Holy Cross area, central Poland, in the Alpine cycle. *Acta Geologica Polonica*, 22: 603–651.

Lamarche, J., Lewandowski, M., Mansy, J. L. & Szulczewski, M., 2003a. Partitioning pre-, syn-and post-Variscan deformation in the Holy Cross Mountains, eastern Variscan foreland. In: McCann, T. & Saintot, A. (eds), *Tracing Tectonic Deformation Using the Sedimentary Record*. *Geological Society, London, Special Publications*, 208: 159–184.

Lamarche, J., Mansy, J., Bergerat, F., Averbuch, O., Hakenberg, M., Lewandowski, M., Stupnicka, E., Świdrowska, J., Wajsprych, B. & Wieczorek, J., 1999. Variscan tectonics in the Holy Cross Mountains (Poland) and the role of structural inheritance during Alpine tectonics. *Tectonophysics*, 313: 171–186.

Lamarche, J., Scheck, M. & Lewerenz, B., 2003b. Heterogeneous tectonic inversion of the Mid-Polish Trough related to crustal architecture, sedimentary patterns and structural inheritance. *Tectonophysics,* 373: 75–92.

Lampe, C., Person, M., Nöth, S. & Ricken, W., 2001. Episodic fluid flow within continental rift basins: some insights from field data and mathematical models of the Rhinegraben. *Geofluids*, 1: 42–52.

Laughland, M. M. & Underwood, M. B., 1993. Vitrinite reflectance and estimates of paleotemperature within the Upper Shimanto Group, Japan. *Geological Society of America Special Paper*, 273: 103–114.

Łuszczak, K., Wyglądała, M., Śmigielski, M., Waliczek, M., Matyja, B. A., Konon, A. & Ludwiniak, M., 2020. How to deal with missing overburden – investigating Late Cretaceous exhumation of the Mid-Polish anticlinorium by a multi-proxy approach. *Marine and Petroleum Geology,* 114: 104229.

Malec, J., 2015. Thermal maturity of Devonian, Carboniferous and Triassic rocks in the central part of the Małopolska Massif from Conodont Colour Alteration Index. *Biuletyn Państwowego Instytutu Geologicznego*, 462: 29–39. [In Polish, with English summary.]

Malec, J., Więcław, D. & Zbroja, S., 2010. The preliminary source rock assessment of the selected Paleozoic deposits of the Holy Cross Mountains. *Geology, Geophysics & Environment*, 36: 5–24.

Marynowski, L., 1999. Thermal maturity of organic matter in Devonian rocks of the Holy Cross Mts. (Central Poland). *Przegląd Geologiczny*, 47: 1125–1129. [In Polish, with English summary.]

Marynowski, L., Czechowski, F. & Simoneit, B. R. T., 2001. Phenylnaphthalenes and polyphenyls in Paleozoic source rocks of the Holy Cross Mountains, Poland. *Organic Geochemistry,* 32: 69–85.

Marynowski, L., Salamon, M. & Narkiewicz, M., 2002. Thermal maturity and depositional environments of organic matter in the post-Variscan succession of the Holy Cross Mountains. *Geological Quarterly,* 46: 25–36.

Marynowski, L., Zatoń, M., Simoneit, B. R. T., Otto, A., Jędrysek, M. O., Grelowski, C. & Kurkiewicz, S., 2007. Compositions, sources and depositional environments of organic matter from the Middle Jurassic clays of Poland. *Applied Geochemistry,* 22: 2456–2485.

Matyja, B. A., 1977. The Oxfordian in the south-western margin of the Holy Cross Mountains. *Acta Geologica Polonica*, 27: 41–64.

Mazur, S., Aleksandrowski, P., Gągała, Ł., Krzywiec, P., Żaba, J., Gaidzik, K. & Sikora, R., 2020. Late Paleozoic strike-slip tectonics versus oroclinal bending at the SW outskirts of Baltica: case of the Variscan belt's eastern end in Poland. *International Journal of Earth Sciences*, 109: 1133–1160.

Mazur, S., Malinowski, M., Maystrenko, Y. P. & Gągała, Ł., 2021. Pre-existing lithospheric weak zone and its impact on continental rifting – The Mid-Polish Trough, Central European Basin System. *Global and Planetary Change*, 198: 103417.

Mazur, S., Mikołajczak, M., Krzywiec, P., Malinowski, M., Buffenmyer, V. & Lewandowski, M., 2015. Is the Teisseyre-Tornquist Zone an ancient plate boundary of Baltica? *Tectonics*, 34: 2465–2477.

Mazur, S., Scheck-Wenderoth, M. & Krzywiec, P., 2005. Different modes of the Late Cretaceous–Early Tertiary inversion in the North German and Polish basins. *International Journal of Earth Sciences*, 94: 782–798.

Mazurek, M., Hurford, A. J. & Leu, W., 2006. Unravelling the multi-stage burial history of the Swiss Molasse Basin: Integration of apatite fission track, vitrinite reflectance and biomarker isomerization analysis. *Basin Research*, 18: 27–50.

McKenzie, D., 1981. The variation of temperature with time and hydrocarbon maturation in sedimentary basins formed by extension. *Earth Planetary Science Letters*, 55: 87–98.

Migaszewski, Z. M., 2002. K-Ar and Ar-Ar dating of diabases and lamprophyres from the Holy Cross Mts. (central Poland). *Przegląd Geologiczny*, 50: 227–229. [In Polish, with English summary.]

Mizerski, W., 2004. Holy Cross Mountains in the Caledonian, Variscan and Alpine cycles – major problems, open questions. *Przegląd Geologiczny,* 52: 774–779. [In Polish, with English summary.]

Mukhopadhyay, P. K., 1992. Maturation of organic matter as revealed by microscopic methods: Applications and limitations of vitrinite reflectance, and continuous spectral and pulsed laser fluorescence spectroscopy. In: Wolf, K. H. & Chilingarian, G. V. (eds), *Diagenesis III. Developments in Sedimentology,* 47: 435–510.

Naglik, B., Toboła, T., Natkaniec-Nowak, L., Luptáková, J. & Milovská, S., 2016. Raman spectroscopic and micro-

thermometric studies of authigenic quartz (the Pepper Mts., Central Poland) as an indicator of fluids circulation. *Spectrochimica Acta Part A: Molecular and Biomolecular Spectroscopy,* 173: 960–964.

Narkiewicz, M., 1991. Mezogenetic dolomitization processes: an example from the Givetian and Frasnian of Holy Cross Mountains, Poland. *Prace Państwowego Instytutu Geologicznego*, 82: 1–54. [In Polish, with English summary.]

Narkiewicz, M., 2002. Ordovician through earliest Devonian development of the Holy Cross Mts. (Poland): constraints from subsidence and thermal maturity data. *Geological Quarterly*, 46: 255–266.

Narkiewicz, M., 2007. Development and inversion of Devonian and Carboniferous basins in the eastern part of the Variscan foreland (Poland). *Geological Quarterly*, 51: 231–256.

Narkiewicz, M., 2017. Comment on a paper by Schito *et al.* (2017) "Thermal evolution of Paleozoic successions of the Holy Cross Mountains (Poland)". *Marine and Petroleum Geology*, 88: 1109–1113.

Narkiewicz, M., 2020. The Variscan foreland in Poland revisited: new data and new concepts. *Geological Quarterly*, 64: 377–401.

Narkiewicz, K. & Malec, J., 2005. Nowa baza danych konodontowego wskaźnika przeobrażeń termicznych (CAI). *Przegląd Geologiczny*, 53: 33–37. [In Polish.]

Narkiewicz, M., Resak, M., Littke, R. & Marynowski, L., 2010. New constraints on the Middle Paleozoic to Cenozoic burial and thermal history of the Holy Cross Mts. (central Poland): results of numerical modeling. *Geologica Acta*, 8: 189–205.

Nawrocki, J., Salwa, S. & Pańczyk, M., 2013. New ^{40}Ar-^{39}Ar age constrains for magmatic and hydrothermal activity in the Holy Cross Mts. (southern Poland). *Geological Quarterly*, 57: 551–560.

Person, M. & Garven, G., 1992. Hydrologic constraints on petroleum generation within continental rift basins: Theory and application to the Rhine Graben. *AAPG Bulletin,* 76: 468–488.

Pieńkowski, G., 2004. The epicontinental Lower Jurassic of Poland. *Polish Geological Institute Special Papers*, 12: 1–154.

Piwocki, M., 2004. Paleogen, Neogen. In: Peryt, M. T. & Piwocki, M. (eds), *Budowa geologiczna Polski, t. I, Stratygrafia, cz. 3a, kenozoik, paleogen, neogen.* Państwowy Instytut Geologiczny, Warszawa, pp. 22–133. [In Polish.]

Poprawa, P. & Żywiecki, M., 2005. Variscan heat transfer along the western prolongation of the Holy Cross Fault Zone by migration of hot fluids related to igneous intrusions (northern Małopolska Block, southern Poland). *Polskie Towarzystwo Mineralogiczne – Prace Specjalne*, 25: 180–183.

Poprawa, P., Żywiecki, M. & Grotek, I., 2005. Burial and thermal history of the Holy Cross Mts. area-preliminary results of maturity modeling. *Polskie Towarzystwo Mineralogiczne – Prace Specjalne*, 26: 251–254.

Pożaryski, W., Grocholski, A., Tomczyk, H., Karnkowski, P. & Moryc, W., 1992. Mapa tektoniczna Polski w epoce waryscyjskiej. *Przegląd Geologiczny,* 40: 643–651. [In Polish.]

Radke, M. & Welte, D. H., 1983. The methylphenanthrene index (MPI): a maturity parameter based on aromatic hydrocarbons. *Advances Organic Geochemistry*, 1981: 504–512.

Resak, M., Glasmacher, U. A., Narkiewicz, M. & Littke, R., 2010. Maturity modeling integrated with apatite fission-track dating: implications for the thermal history of the Mid-Polish Trough (Poland). *Marine & Petroleum Geology*, 27: 108–115.

Resak, M., Narkiewicz, M. & Littke, R., 2008. New basin modeling results from the Polish part of the Central European Basin system: implications for the Late Cretaceous–Early Paleogene structural inversion. *International Journal of Earth Sciences,* 97: 955–972.

Sakaguchi, A., Yanagihara, A., Ujiie, K., Tanaka, H. & Kameyama, M., 2007. Thermal maturity of a fold-thrust belt based on vitrinite reflectance analyzis in the Western Foothills complex, western Taiwan. *Tectonophysics*, 443: 220–232.

Schegg, R. & Leu, W., 1998. Analyzis of erosion events and palaeogeothermal gradients in the North Alpine Foreland Basin of Switzerland. *Geological Society, London, Special Publications*, 141: 137–155.

Schito, A., Corrado, S., Trolese, M., Aldega, L., Caricchi, C., Cirilli, S., Grigo, D., Guedes, A., Romano, C., Spina, A. & Valentim, B., 2017. Assessment of thermal evolution of Paleozoic successions of the Holy Cross Mountains (Poland). *Marine and Petroleum Geology*, 80: 112–132.

Schlumberger, 2023. *PetroMod 1-D software*. https://www.slb.com/products-and-services/delivering-digital-at-scale/software/petromod-basin-modeling-software/petromod [17.11.2023]

Senglaub, Y., Brix, M. R., Adriasola, A. C. & Littke, R., 2005. New information on the thermal history of the southwestern Lower Saxony Basin, northern Germany, based on fission track analysis. *International Journal of Earth Sciences,* 94: 876–896.

Słaby, E., Breitkreuz, C., Żaba, J., Domańska-Siuda, J., Gaidzik, K., Falenty, K. & Falenty, A., 2010. Magma generation in an alternating transtensional–transpressional regime, the Kraków–Lubliniec Fault Zone, Poland. *Lithos*, 119: 251–268.

Smolarek, J., Marynowski, L., Spunda, K. & Trela, W., 2014. Vitrinite equivalent reflectance of Silurian black shales from the Holy Cross Mountains, Poland. *Mineralogia*, 45: 79–96.

Sobczyk, A., Sobel, E. & Georgieva, V., 2020. Meso–Cenozoic cooling and exhumation history of the Orlica-Śnieżnik Dome (Sudetes, NE Bohemian Massif, Central Europe): Insights from apatite fission-track thermochronometry. *Terra Nova*, 32: 122–133.

Środoń, J. & Trela, W., 2012. Preliminary clay mineral data on burial history of the Holy Cross Mts., Poland. *Mineralogia – Special Papers*, 39: 93–94.

Suarez-Ruiz, I., Flores, D., Mendonca, J. G. & Hackley, P. C., 2012. Review and update of the application of organic petrology: Part 1 – geological applications. *International Journal of Coal Geology*, 99: 54–112.

Suchý, V., Filip, J., Sýkorová, I., Pešek, J. & Kořínková, D., 2019. Palaeo-thermal and coalification history of Permo-Carboniferous sedimentary basins of Central and Western Bohemia, Czech Republic: first insights from apatite fission track analyzis and vitrinite reflectance modeling. *Bulletin of Geosciences*, 94: 201–219.

Summer, N. S. & Verosub, K. L., 1992. Diagenesis and organic maturation of sedimentary rocks under volcanic strata, Oregon. *AAPG Bulletin,* 76: 1190–1199.

Swadowska, E., 2006a. Petrograficzna charakterystyka rozproszonej materii organicznej**.** In: Kowalczewski, Z. (ed.), *Opoczno PIG-2. Profile głębokich otworów wiertniczych Państwowego Instytutu Geologicznego*, 111: 73–75. [In Polish.]

Swadowska, E., 2006b. Wyniki badania materii organicznej. In: Kowalczewski, Z. (ed.), *Ostałów PIG-2. Profile głębokich otworów wiertniczych Państwowego Instytutu Geologicznego*, 112: 76–78. [In Polish.]

Sweeney, J. J. & Burnham, A. K., 1990. Evaluation of a simple model of vitrinite reflectance based on chemical kinetics. *AAPG Bulletin*, 74: 1559–1570.

Szafran, S. & Wagner, M., 2000. Geotektoniczne przyczyny zmian średniej refleksyjności huminitu/witrynitu w materii organicznej miocenu w zapadlisku przedkarpackim. *Zeszyty Naukowe Politechniki Śląskiej – Seria Górnictwo,* 246: 517–532. [In Polish.]

Szaniawski, R., 2008. Late Paleozoic geodynamics of the Małopolska Massif in the light of new paleomagnetic data for the southern Holy Cross Mountains. *Acta Geologica Polonica*, 58: 1–12.

Szczepanik, Z., 1997. Preliminary results of thermal alteration investigations of the Cambrian acritarchs in the Holy Cross Mts. *Geological Quarterly,* 41: 257–264.

Szczepanik, Z., 2001. Acritarchs from Cambrian deposits of the southern part of the Łysogory unit in the Holy Cross Mountains, Poland. *Geological Quarterly,* 45: 117–130.

Tobin, R. C. & Claxton, B. L., 2000. Multidisciplinary thermal maturity studies using vitrinite reflectance and fluid inclusion microthermometry: a new calibration of old techniques. *AAPG Bulletin*, 84: 1647–1665.

Turnau, E., 1999. *Rezultaty badań palinostratygraficznych osadów karbonu z otworów Ostałów PIG-2 i Opoczno PIG-2*. Centralne Archiwum Geologiczne Państwowego Instytutu Geologicznego, Warszawa, 127 pp. [In Polish.]

Waples, D. W., Kamata, H. & Suizu, M., 1992a. The art of maturity modeling, part 1: finding of a satisfactory model. *AAPG Bulletin,* 76: 31–46.

Waples, D. W., Kamata, H. & Suizu, M., 1992b. The art of maturity modeling, part 2: alternative models and sensitivity analyzis. *AAPG Bulletin,* 76: 47–66.

Willett, S. D. & Chapman, D. S., 1987. Temperatures, fluid flow and thermal history of the Uinta Basin. In: Doligez, B. (ed.), *Migration of Hydrocarbons in Sedimentary Basins.* Editions Technip, Paris, pp. 533–551.

Yamaji, A., 1986. Analysis of vitrinite reflectance-burial depth relations in dynamical geological settings by direct integration method. *Journal of Japan Association of Petroleum Technology,* 51: 1–8.

Żakowa, H. & Migaszewski, Z., 1995. Holy Cross Mountains. In: Zdanowski, A. & Żakowa, H. (eds), *The Carboniferous system in Poland. Prace Państwowego Instytutu Geologicznego*, 148: 109–115.

Ziagos, J. P. & Blackwell, D. D., 1986. A model for the transient temperature effects of horizontal fluid flow in geothermal systems. *Journal of Volcanology and Geothermal Research*, 27: 371–397.

Ziegler, P. A. & Dèzes, P., 2007. Cenozoic uplift of Variscan massifs in the Alpine foreland: Timing and controlling mechanisms. *Global & Planetary Change*, 58: 237–269.

Zwing, A., 2003. *Causes and Mechanisms of Remagnetisation in Paleozoic Sedimentary Rocks – A Multidisciplinary Approach*. Ph.D. Thesis. Fakultät für Geowissenschaften der Ludwig-Maximilians-Universität München, 172 pp.